



A novel strategy for multi-part production in additive manufacturing

Jingchao Jiang^{1,2} · Xun Xu¹ · Yi Xiong² · Yunlong Tang³ · Guoying Dong² · Samyeon Kim²

Received: 9 February 2020 / Accepted: 6 July 2020 / Published online: 13 July 2020
© Springer-Verlag London Ltd., part of Springer Nature 2020

Abstract

In this paper, a novel strategy for multi-part additive manufacturing (AM) production is proposed in order to reduce the total fabrication time. Traditionally, in a multi-part production process, parts are positioned on the print platform and then are sliced into layers from the bottom to the top. In this manner, the time for moving the print nozzle from one part to another in each layer can be excessive. In fact, it is possible to fabricate some more layers (instead of one layer) in the same part first, before moving to another part to start printing. Based on this idea, parts need to be positioned on the platform optimally. The best positions are determined by considering and calculating the total fabrication time. An eight-step novel strategy is proposed in this paper to obtain parts' optimal positions and nozzle travel paths. A case study was carried out to demonstrate that this strategy can save fabrication time for multi-part manufacturing in AM, compared with normal multi-part fabrication method.

Keywords Additive manufacturing · Multi-part production · Optimization

1 Introduction

Additive manufacturing (AM) technologies (also known as rapid prototyping, 3D printing, solid freeform fabrication, etc.) can fabricate complex parts with theoretically any shape, compared with traditional manufacturing techniques [1]. With this advantage, AM has currently been used in many fields, including industrial, marine, aerospace, and daily supplies. AM techniques can be divided into seven types: (i) material extrusion, (ii) powder-bed fusion, (iii) material jetting, (iv) binder jetting, (v) directed energy deposition, (vi) vat photopolymerization, and (vii) sheet lamination [2]. Among them, material extrusion-based AM is widely used nowadays due to its simplicity and low cost [3]. A wide variety of materials can be extruded in this technique, thermoplastics are the most popular, such as acrylonitrile butadiene styrene (ABS),

high-impact polystyrene (HIPS), polylactic acid (PLA), thermoplastic polyurethane (TPU), aliphatic polyamides (PA, also known as Nylon), and more recently gelatin methacryloyl (GelMA) [4–6]. In addition, paste-like materials such as chocolate, ceramics, and concrete can also be used for extrusion in this technique [7–9]. A typical process of material extrusion-based AM is illustrated in Fig. 1. The 3D model of the product is first sliced into layers; then, the support needs to be generated for successful fabrication [10, 11]. Finally, the extrusion-based AM machine will manufacture the product in a layer-by-layer manner from the product bottom to the top, as shown in Fig. 1. The material is extruded from the print nozzle and then positioned on the platform. The platform moves one-layer height down after finishing each layer fabrication until the whole product is completed.

The movements of the print nozzle, also called print path or tool path in AM, can be optimized or designed with specific aims. Ding et al. [12] proposed a practical path planning strategy for fabricating thin-walled structures in wire and arc AM process. Jin et al. [13] optimized tool path generation in extrusion-based AM for improving efficiency and precision. They also proposed a non-retraction path planning strategy for improving the efficiency in extrusion-based AM [14]. Toolpaths for printing functionally graded materials (FGM) parts were proposed by Muller et al. [15] in an additive laser melting system. Similarly, Ozbolat and Khoda [16] proposed a new parametric path planning method for printing hollow

✉ Jingchao Jiang
jjia547@aucklanduni.ac.nz

¹ Department of Mechanical Engineering, University of Auckland, Auckland 1142, New Zealand

² Digital Manufacturing and Design Center, Singapore University of Technology and Design, Singapore, Singapore

³ Department of Mechanical and Aerospace Engineering, Monash University, Clayton, Victoria 3800, Australia

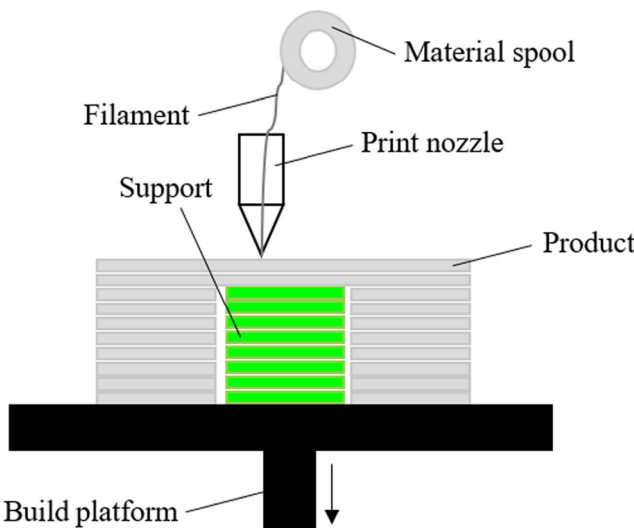


Fig. 1 Typical extrusion AM process

porous structures with functionally graded materials in AM. A hybrid deposition path planning method was proposed by Liu et al. [17] for printing lightweight and topologically optimized parts in extrusion-based AM. Coupek et al. [18] proposed a path planning algorithm to reduce support usage and building time in multi-axis AM processes. We previously also developed new support strategies based on print path optimization for reducing support material waste [19, 20]. We also proposed a support interface method for easy part removal in AM through print path optimization [21].

Generally, in extrusion-based AM processes, parts are fabricated one by one in each manufacturing circle. Currently, for improving product development and saving fabrication time, the way of multiple parts fabricated in the same chamber in one AM process has been applied in some applications. Zhang et al. [22] developed a two-step method to solve the orientation optimization problem for multi-part fabrication at the

same time, where a group of parts in the same build vat or chamber are optimally orientated simultaneously. Jiang et al. [23] proposed an improved method to fabricate multiple parts at the same time considering support material consumption. However, both the above papers did not consider the fact that all parts do not need to be printed by keeping the same height of printed layers in each part. The bottom layer of the first part can be printed first, then still printing only in this part for several layers. After this, the print nozzle moves from the current part to the most bottom layer of next part, then starting printing layers from the bottom for several layers, then the print nozzle moves to the next part or moves back to the first part continuing the rest of the first part if there is no third part existing. Figure 2 shows an example for illustration. Traditionally, as shown in Fig. 2a, 3D models of parts 1 and 2 are sliced into layers for fabrication as shown in Fig. 2b which is a traditional way. The print path moves through A1-B1-A2-B2-A3-B3-A4-B4. In this paper, we propose that these two parts do not need to be kept in the same layer for printing. As shown in Fig. 2c, part 1 (four layers) can be finished first, then printing part 2. The print path moves through B1-A1-B2-A2-B3-A3-B4-A4-A5-B5-A6-B6-A7-B7-A8-B8. It can be seen that the strategy in Fig. 2c has a shorter total path length than that in Fig. 2b, thus saving total fabrication time. However, this is based on the assumption that the nozzle can move freely between parts. In real cases, the nozzle is not always able to move freely between parts. The details of how this works will be explained in the next section. The proposed strategy for multi-part production in this paper mainly consists of eight steps which will also be illustrated in the next section. This new strategy for multi-part production can save total fabrication time, thus enhancing the development circle of products and reducing AM machine energy consumption. A case study with three parts was carried out in this paper to validate the proposed strategy.

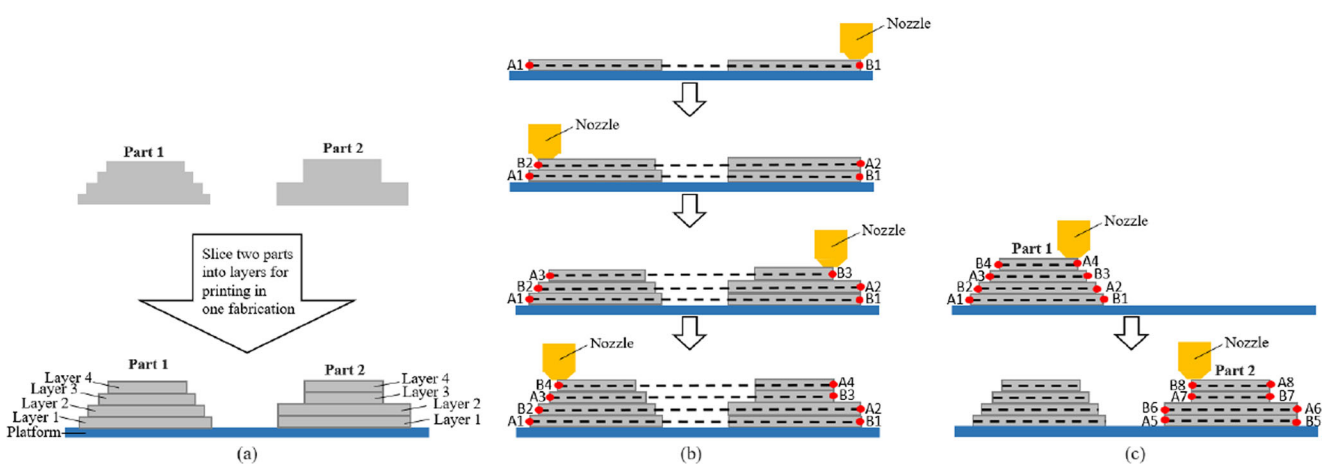


Fig. 2 **a** Slice two parts into layers for printing; **b** traditional way for printing two parts; **c** simplified illustration of the proposed strategy for printing two parts

2 Methodology

In this section, our proposed strategy for multi-part production is explained in detail. The strategy consists of eight steps. Before illustrating this strategy, some background will be introduced first.

2.1 Background

2.1.1 Why is it possible to fabricate one part for several layers, then moving to another part?

The reason for this is because the nozzle package part of each AM machine has some spare space beneath it. For example, in Delta 3D printer as shown in Fig. 3, the nozzle package has some spare space outside the heater, nozzle, and connection structure. Therefore, even the first part has several layers printed; it will not influence the next part fabrication if the total printed layer height of the first part sits within the spare space of the nozzle package. Figure 4 a shows an example of this case (note that parts a and b in Fig. 4 are just parts with some layers for illustration). However, it is not possible to fabricate the next part if the first part has too many layers printed whose total height is larger than the threshold and thus out of the spare space of the nozzle package, as shown in Fig. 4b. In a case like that, there are two ways to make this still possible to be printed. Figure 4 c shows one solution by splitting the first part into several times of “several layer printing,” the print strategy is to move the nozzle along 1-2-3-4-5-6-7-8-9-10-11-12-13-14-15-16. Another solution is shown in Fig. 4d by increasing the distance between two parts; thus, the first part can have more printed layers as the spare space increases, the nozzle moves along 1-2-3-4-5-6-7-8-9-10-11-12-13-14-

15-16. As can be seen in Fig. 5, the spare space increases as the distance between parts increases. The method to adopt this and find the best strategy among them for multi-part production will be illustrated later. Note that different AM machines have different structures and need their own specific analysis for optimization. In this paper, only the Kossel Delta 3D printer is used for demonstration and illustration.

2.1.2 Fabrication direction optimization for each part

In AM, print orientation/direction is an important factor that influences the support material waste, fabrication time, and final printed properties. Figure 6 shows an example; no support structure is needed in the direction 2 of the “T” part. While for the print direction 1, support material which is wasted after fabrication is necessary. A variety of studies have been carried out with the aim of finding an optimal direction for a single part [24–28]. Based on the above existing knowledge, the direction of every single part can be optimized. In our strategy steps illustrated later, once selecting a part, that part has already been optimized in terms of print direction.

2.2 Proposed strategy for multi-part production

The proposed strategy for multi-part production will be illustrated in this sub-section. This strategy consists of eight steps as shown in Fig. 7.

Step 1: Select one part as the first part In this step, select one part as the first part.

Step 2: Position this part at the middle left of the platform Position the first part at the middle left of the platform. This is

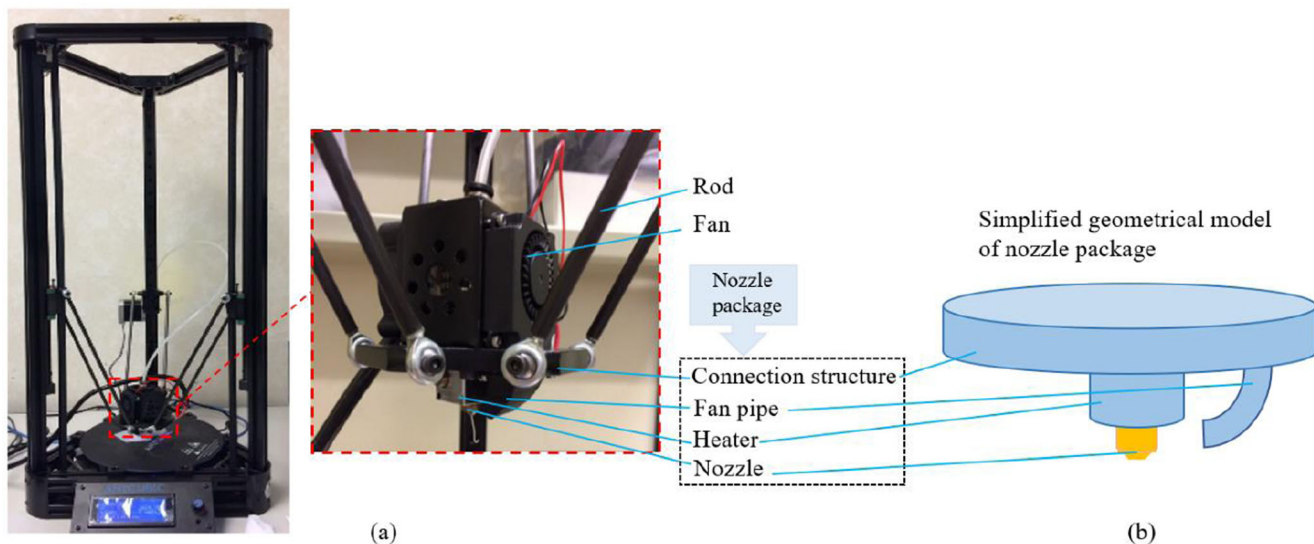


Fig. 3 Delta printer nozzle package structure (a) and its simplified 3D model (b)

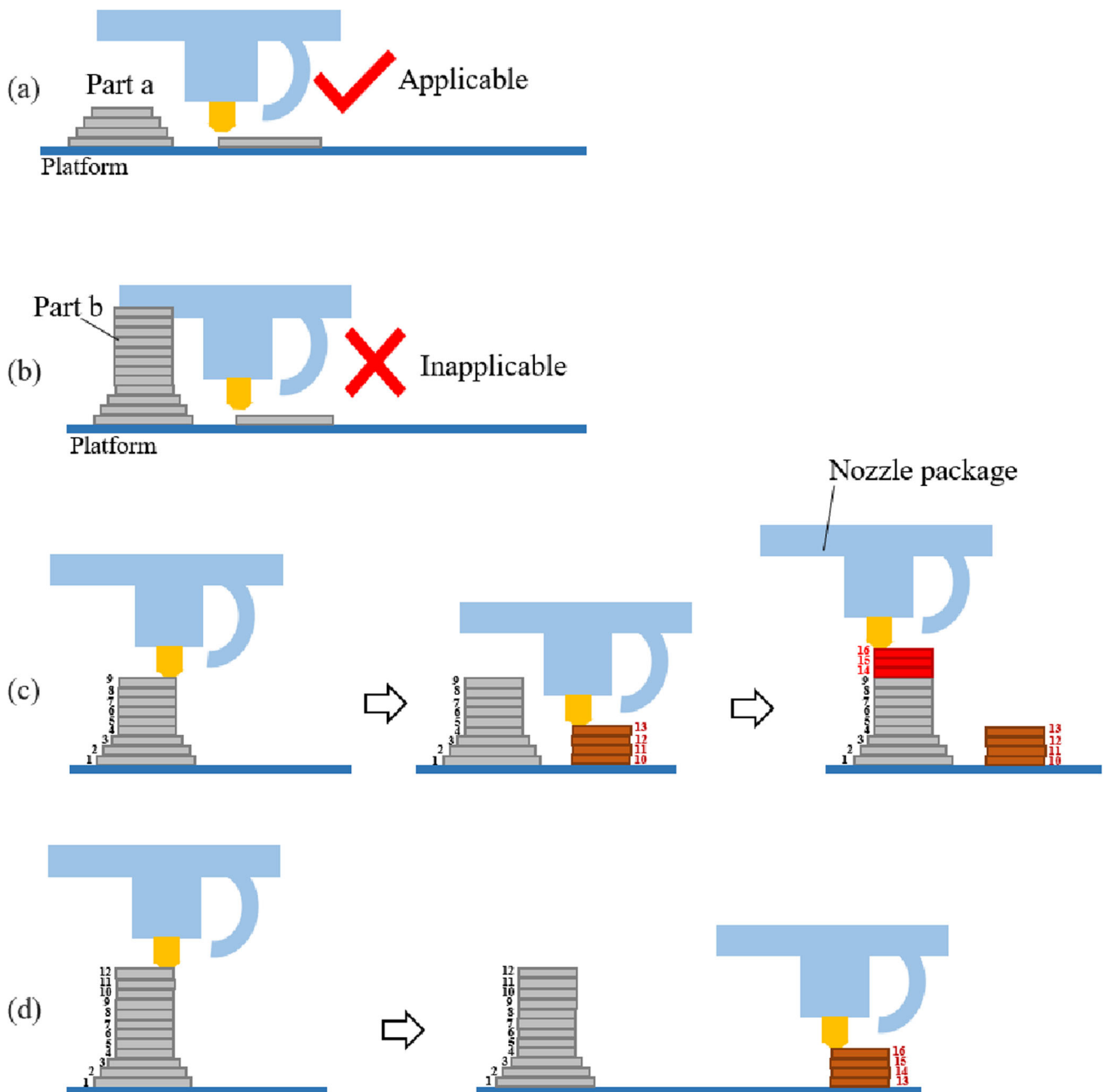


Fig. 4 Demonstration of different cases. **a** An example of the applicable case; **b** an example of the inapplicable case; **c, d** two applicable cases with different strategies

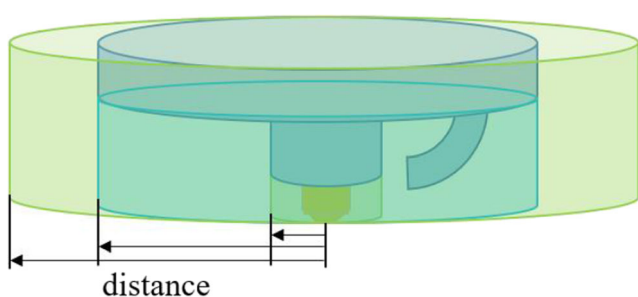
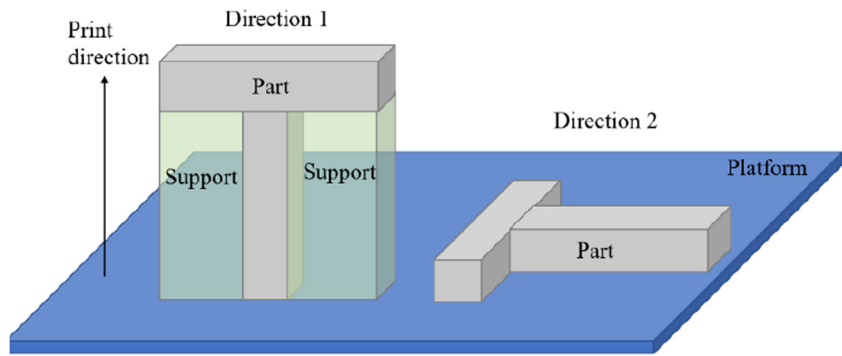


Fig. 5 Illustration of spare space increase as the distance between parts increases

because the print nozzle is set to start from the left to the right for all parts as there is a fan pipe on the right of the nozzle package as shown in Fig. 3a. Therefore, the right position of the nozzle package has no effect on the left spare space if the nozzle moves from the left to the right. In this paper, the strategy of multi-part production does not consider the right spare space of the nozzle package in the optimization process, for easy analysis. Only the left spare space of the nozzle package will be used for optimization. Note that, this depends on the structure of the AM machine. For different AM machines, the structure sizes and details might be different.

Fig. 6 Two print directions of the same “T” part



Step 3: Select a second part

Step 4: Change the position of the second part and find the best position Once a second part is selected. This part can be positioned anywhere on the platform next to the first part. The next thing is to find the best position for the second part. First of all, these two parts should not be positioned with any

overlapped areas as shown in Fig. 8a, which makes it hard or even impossible to divide these two parts away. To achieve this, the contours of each part in the same sliced layer should not have an overlapped area. Figure 8 b shows a feasible example position in 3D, while Fig. 8c shows more feasible positions in 2D (top view). The next step is to find which position of part 2 is the best. Therefore, the whole part

Fig. 7 Steps of the proposed strategy for multi-part production

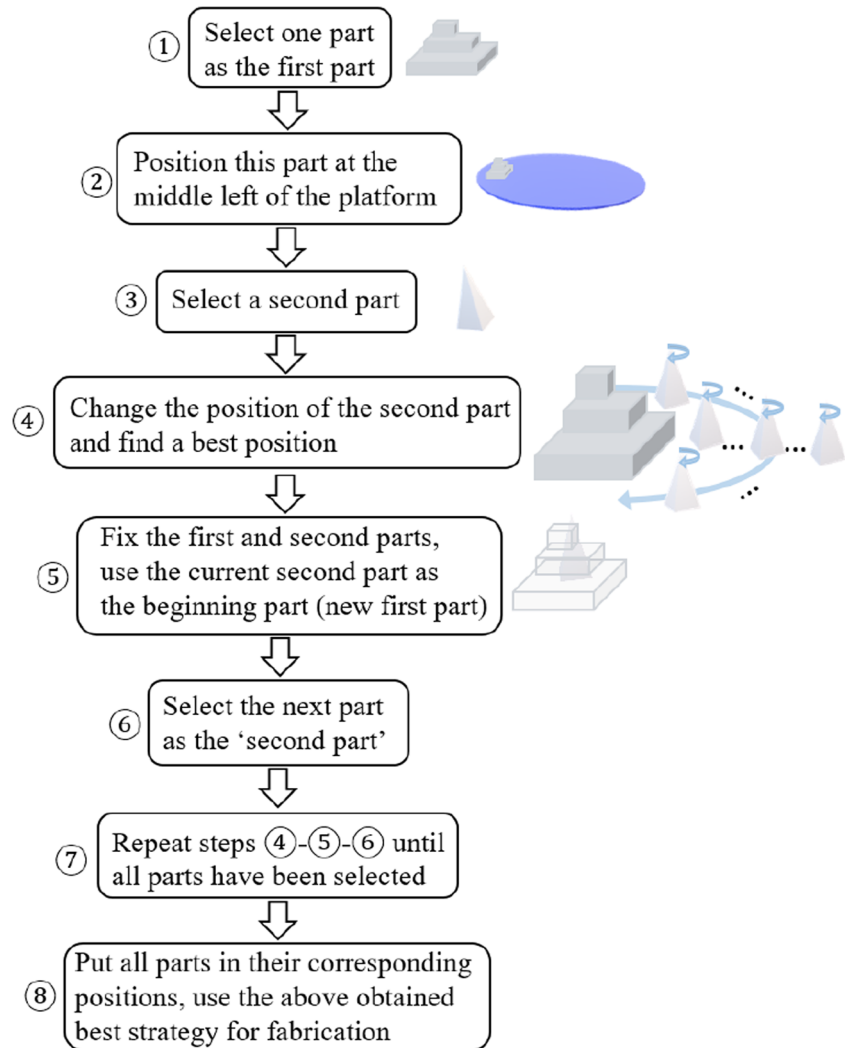
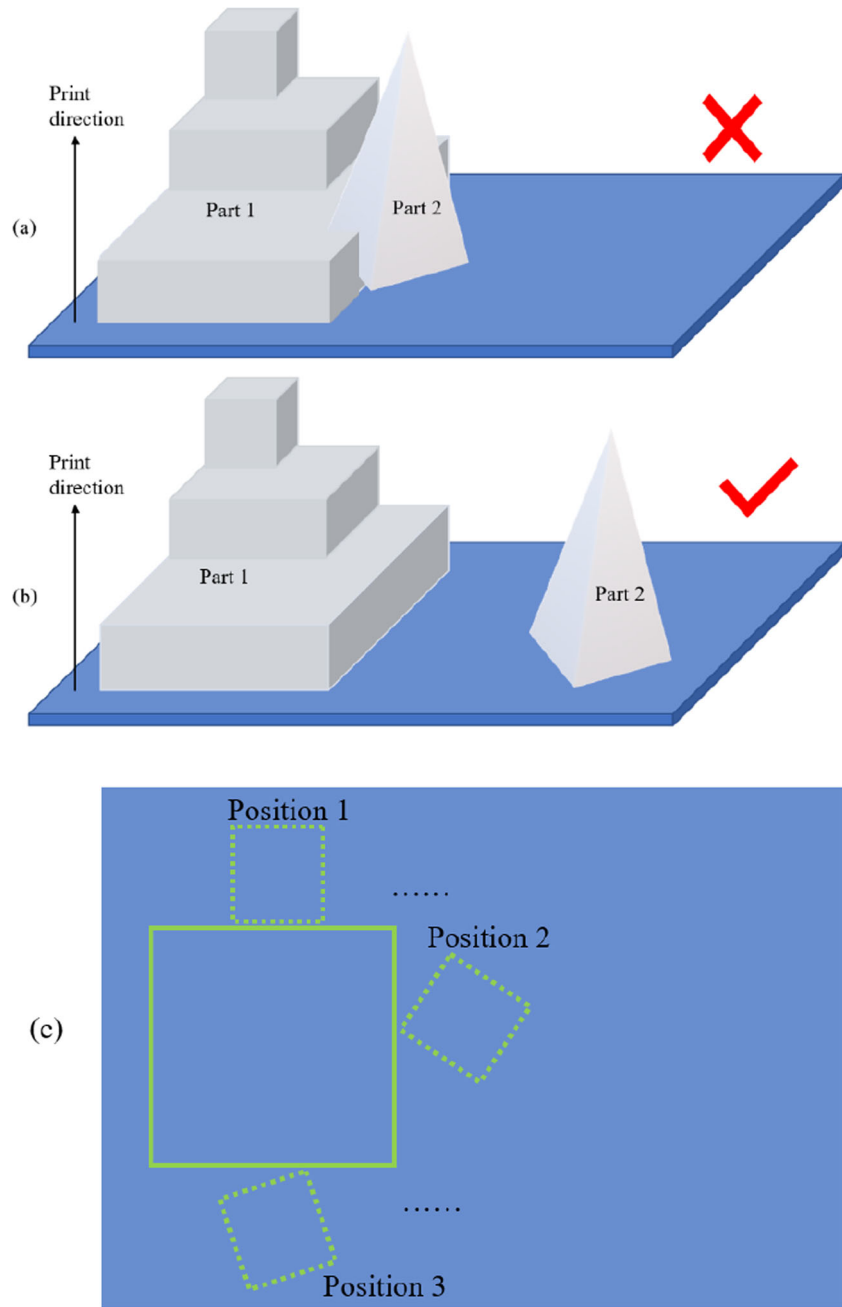


Fig. 8 **a** Two parts positioned with the overlapped area; **b** an example of a feasible position of part 2; **c** more feasible positions (top view)



structure needs to be considered now for comparison among feasible positions of part 2.

To find the best position of part 2, the total fabrication time is used as the objective to minimize. The time for printing the inside of each part should have no difference in different part positions. The main influential fact that affects the total fabrication time is the time used for nozzle traveling between parts. Therefore, only the total time spent on nozzle moving between parts needs to be calculated and compared. Figure 9 shows an example of how to calculate the time. As illustrated in Fig. 4, providing the safe total height of printed layers in each movement

between parts is set at h . The safe height h can be $h_{\text{nozzle}} + h_{\text{heater}}$ or $h_{\text{nozzle}} + h_{\text{heater}} + h_{\text{structure}}$ as shown in Fig. 10, depending on the distance between parts as illustrated in Fig. 5. Once the value of h is set, the total time spent on travel between parts can be calculated as follows:

$$t = \frac{\sum_{i=0}^n l^i}{v_{\text{nozzle}}} \quad (1)$$

where n is the total number of sliced travel times between parts and l^i means the total nozzle travel length between parts

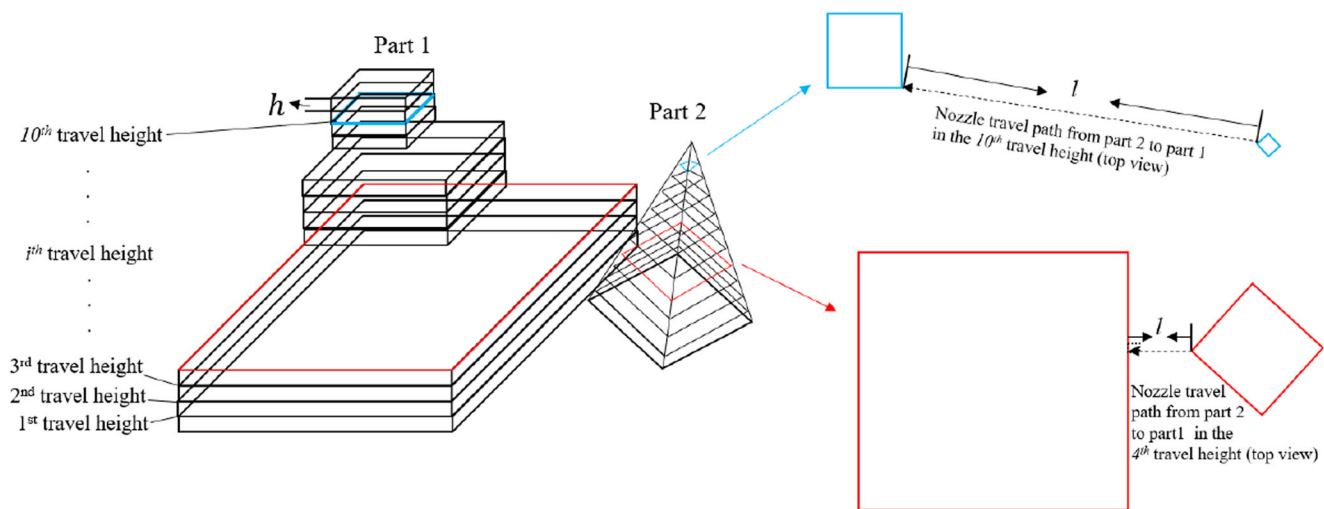


Fig. 9 Examples of sliced parts by the height of h , travel distance (l) between parts, and i th travel height

in the i th travel height. The meaning of i th travel height is shown on the left in Fig. 9. v_{nozzle} is the nozzle move speed between parts. t is the total time spent on moving between these two parts.

Based on Eq. (1), corresponding t can be calculated in different positions of part 2. Then, the position which spends the least time t will be chosen as the best position. Note that once moving the position of part 2, the distance illustrated in Fig. 5 will be changed; thus, the value of h can be changed correspondingly. Figure 11 shows the algorithm for obtaining the best part position and nozzle travel paths between every two parts.

Step 5: Fix the first and second parts, use the current second part as the beginning part (new first part) In this step, the second part position has been optimized and needs to be fixed for optimizing the next part. This second part will be marked as the “first part” for circling the above process for optimization.

Step 6: Select the next part as the “second part” Similarly, take the next part as the “second part” for optimization.

Step 7: Repeat steps 4, 5, and 6 until all parts have been selected

Step 8: Put all parts in their corresponding positions, use the above obtained best strategy for fabrication Once all the parts are optimally positioned on the platform, the print path (print nozzle move path) will be generated based on the final best strategy and then sent to extrusion-based AM machines for fabrication. The exact path connecting different parts and the connection points in each part are fixed as optimized, while the paths inside each part itself can be changed or optimized as the customer’s wish. As illustrated in the introduction of this paper, all the previous studies on print path optimization with different aims can be used inside each part in the multi-part production process. The only difference is to accurately connect each part along the optimized connection paths and points.

3 Case study and discussion

In this section, a case study is used to further illustrate and demonstrate the details of the proposed strategy. A Kossel Delta 3D printer was used as the aim AM machine (shown in Fig. 3a). Therefore, the nozzle package sizes of this machine were used for multi-part production optimization. The corresponding sizes of this machine are as follows: $h_{\text{nozzle}} = 8$ mm, $h_{\text{heater}} = 18$ mm, $h_{\text{structure}} = 10$ mm, $d_{\text{heater}} = 9$ mm, and

Fig. 10 Illustration of h_{nozzle} , h_{heater} , $h_{\text{structure}}$, $d_{\text{structure}}$, and d_{heater}

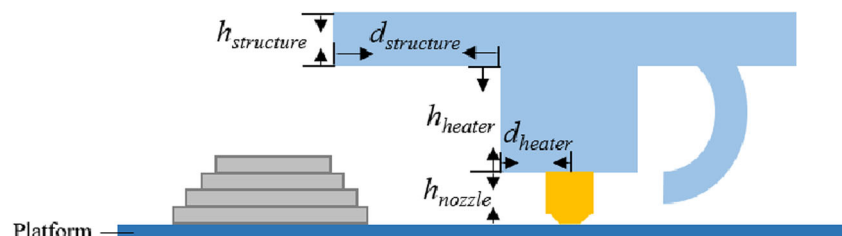
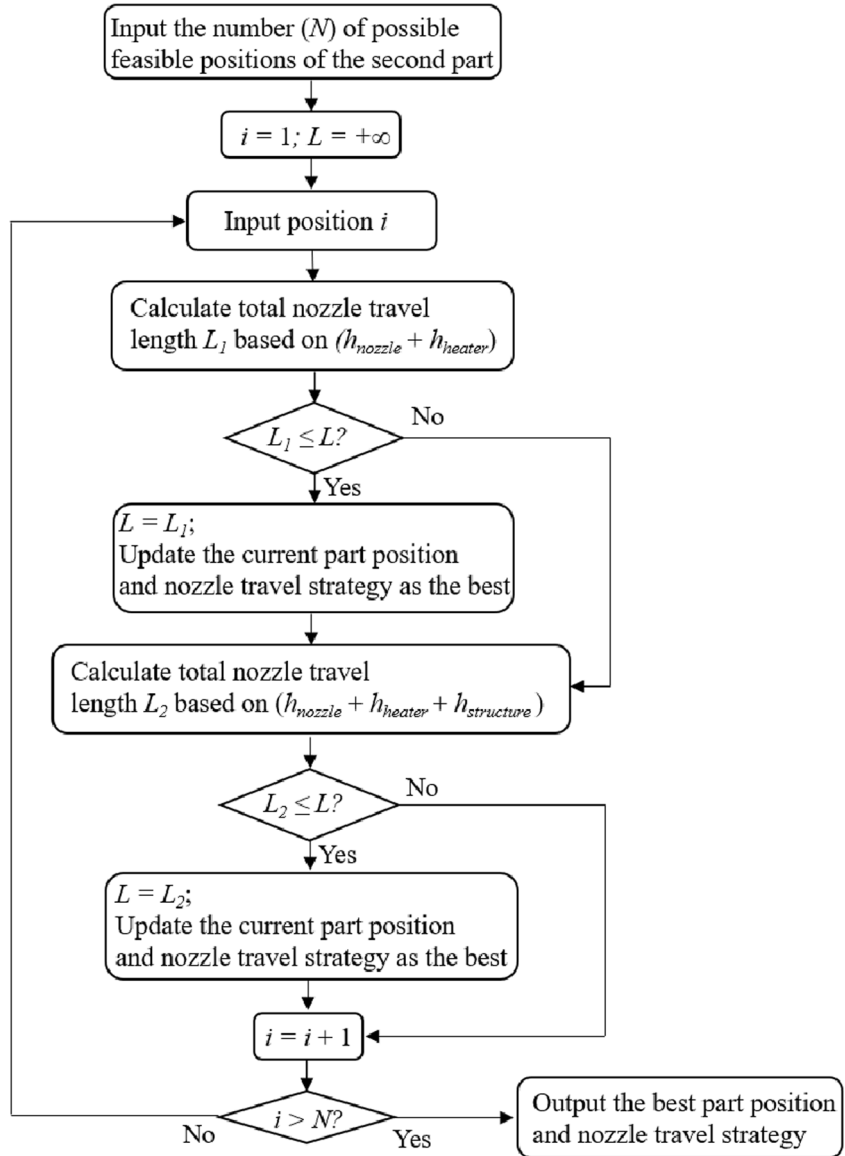


Fig. 11 Algorithm for obtaining best part position and nozzle travel strategy in every two parts



$d_{\text{structure}} = 30$ mm. For making the demonstration clear and easy to be understood, only three simple parts were chosen and demonstrated in this case study. The sizes of these three parts are shown in Fig. 12. After using the strategy proposed in Section 2, the best positions of the three parts for fabrication are shown in Fig. 13a (Fig. 13b shows the positions in a top view). Note that part c needs support structures for successful fabrication; thus, the support structure areas were considered as a part of part c when using the strategy proposed in Section 2. The support structure areas were generated based on setting the printable threshold overhang angle size at 45° [29]. For clearly showing the nozzle travel paths between parts, 2D illustration is used instead of 3D. Figure 14 a and b show two strategies of the nozzle travel paths between parts a and b, while Fig. 14 c and d show that between parts b and c (based on the distance of $(d_{\text{heater}} + 0.4)$ mm) or $(d_{\text{heater}} +$

$d_{\text{structure}} + 0.4$ mm), respectively). The reason for “+ 0.4 mm” is to further avoid the colliding between nozzle and parts when the nozzle is traveling between parts. In the position of Fig. 14a, the safe total height in each travel between parts can be set as $(h_{\text{nozzle}} + h_{\text{heater}} - 0.4)$ mm. The reason for “− 0.4 mm” is to further ensure safe fabrication without colliding between nozzle and parts. Therefore, h is set at 25.6 mm. Then, the nozzle travel paths between parts (red arrows) can be obtained as shown in Fig. 14a. The sequence is as follows: ①-②-③-④-⑤-⑥-⑦-⑧-⑨-⑩-⑪. Similarly, in Fig. 14b, h is set at $(h_{\text{structure}} + h_{\text{nozzle}} + h_{\text{heater}} - 0.4 = 35.6)$ mm and the nozzle travel paths between parts (red arrows) can be obtained as shown (red arrows). The sequence is as follows: ①-②-③-④-⑤-⑥-⑦-⑧. The total corresponding nozzle travel path length L between parts a and b can be calculated as follows:

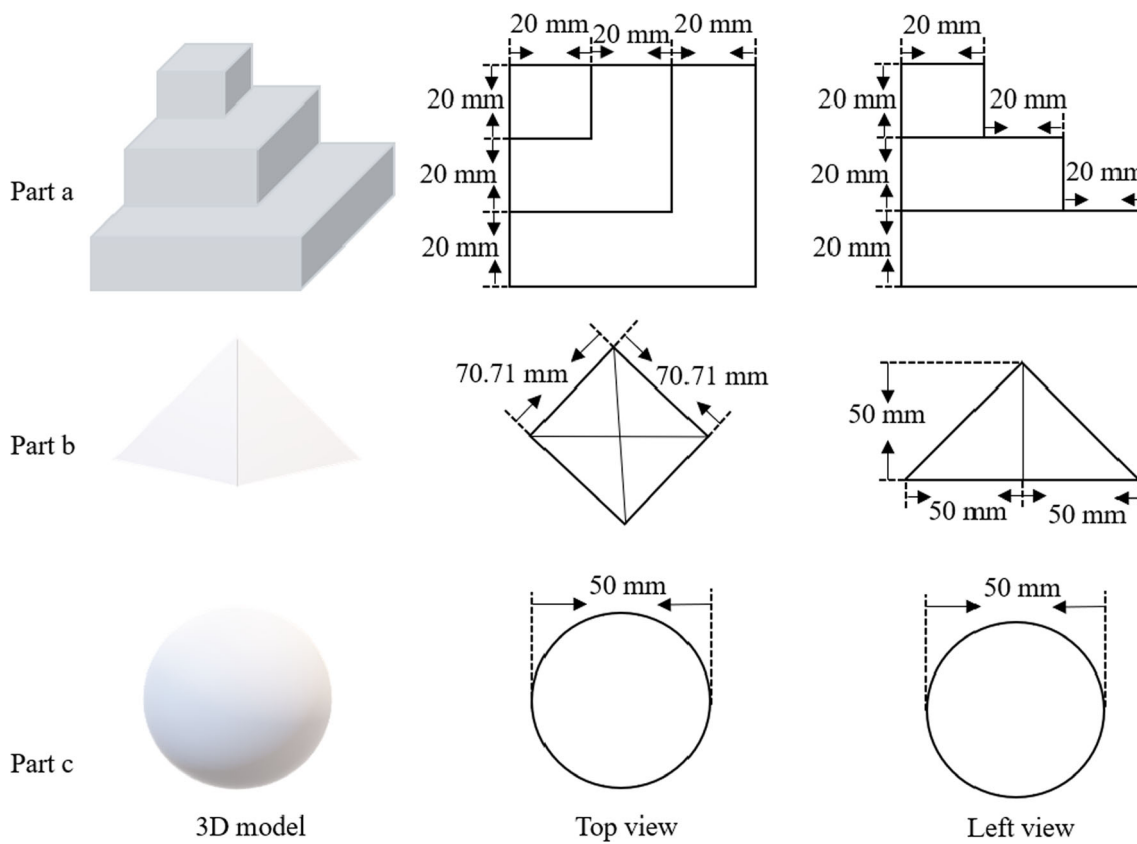


Fig. 12 Parts used in the case study

$$\begin{cases} \text{Fig.14(a)} & L = \sum_{j=1}^7 l_j = 161.55 \text{ mm} \\ \text{Fig.14(b)} & L = \sum_{j=1}^5 l_j = 228.54 \text{ mm} \end{cases} \quad (2)$$

Based on the results of Eq. (2), the position and strategy in Fig. 14a should be chosen as it has a shorter nozzle travel length than that in Fig. 14b. After analysis, similarly, the position and strategy in Fig. 14c should be chosen for parts b and

c. Then, combine the above two, the best positions and nozzle travel paths for all three parts can be obtained. Note that the nozzle paths inside each part are not the focus of this paper as the time spent on inside paths moving is the same in different strategies.

With the aim of comparing our strategy with the traditional method, Cura 4.1.0 was used to slice the three parts and estimate the fabrication time for the traditional multi-part production method, using this Kossel Delta 3D printer. The slicing

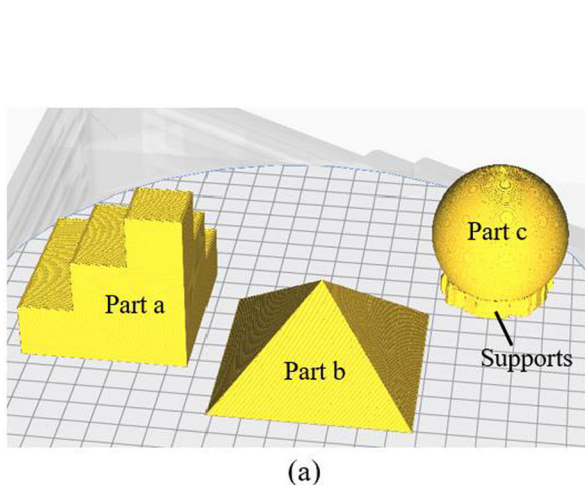
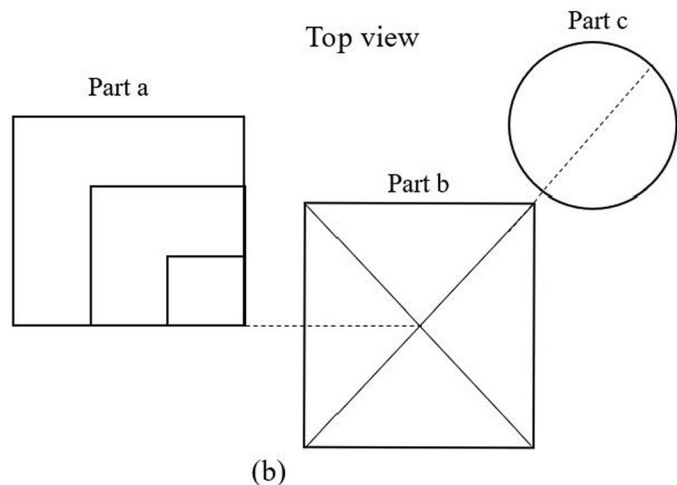


Fig. 13 Best positions of the three parts in our strategy



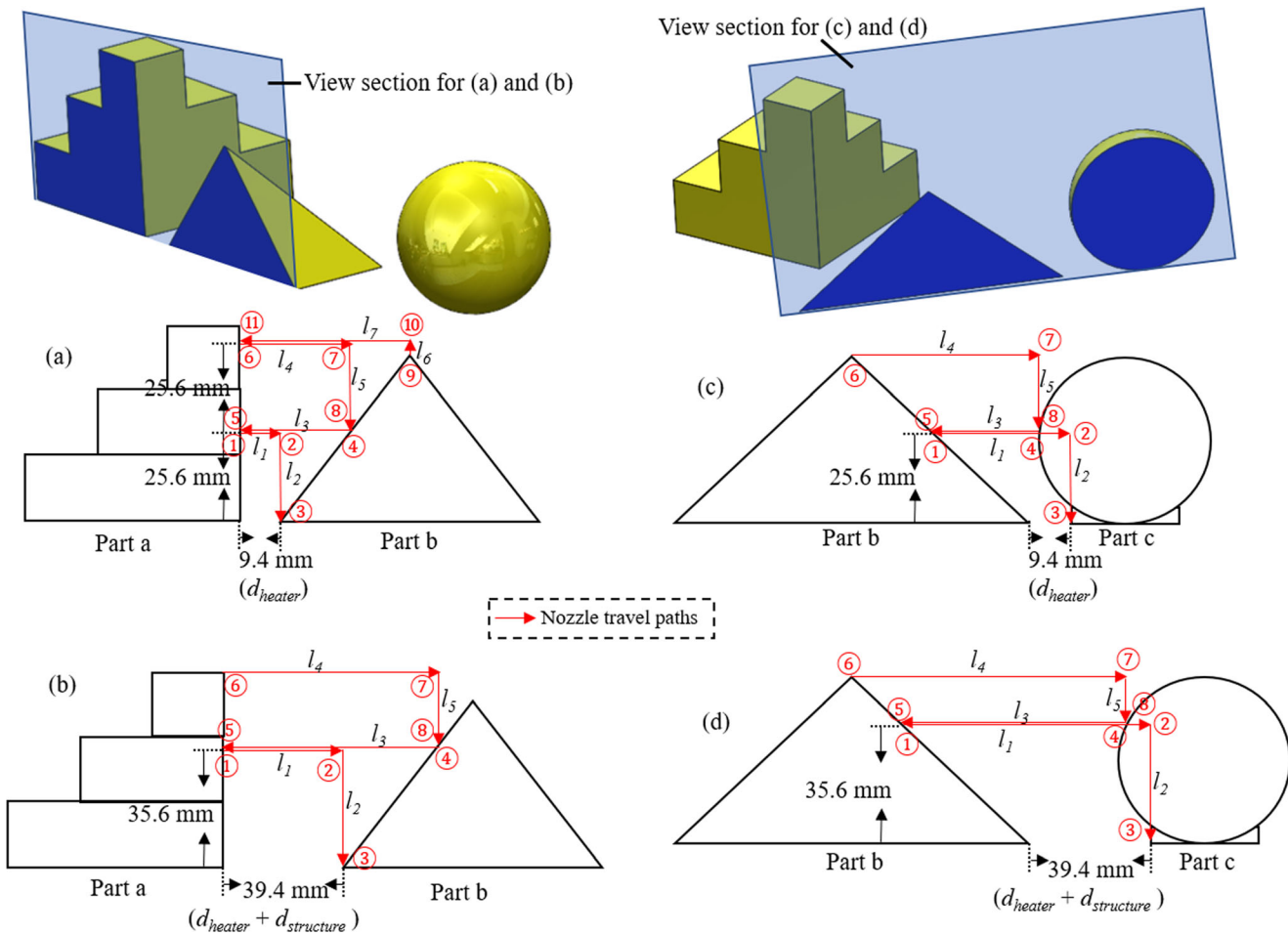


Fig. 14 Nozzle travel paths between parts a and b based on ($d_{\text{heater}} + 0.4$) (a) and ($d_{\text{heater}} + d_{\text{structure}} + 0.4$) (b); nozzle travel paths between parts b and c based on ($d_{\text{heater}} + 0.4$) (c) and ($d_{\text{heater}} + d_{\text{structure}} + 0.4$) (d)

parameters used are listed in Table 1. The three parts were positioned as close as possible to save the nozzle travel time between parts. The corresponding best positions are shown in Fig. 15. In our proposed strategy, we changed the nozzle travel paths between parts as illustrated in Fig. 14 a and c, while keeping all the other parameters the same as Table 1. The corresponding fabrication time of the traditional method and

our proposed strategy is shown in Table 2. As can be seen, our proposed strategy can save 149 s in terms of time spent on printing the three parts.

In fact, this strategy can also be used for single part fabrication if that part has “multi-part” features. “Multi-part” feature means that a single component has some independent parts which can be seen as different components in a specific range of height. Figure 16 shows two examples.

Table 1 Slicing parameters set for slicing the three parts in Cura 4.1.0

Parameters	Value
Layer height	0.1 mm
Wall thickness	0.8 mm
Top/bottom thickness	0.8 mm
Infill pattern	Lines with 20% infill
Print speed	30 mm/s
Nozzle travel speed	120 mm/s
Support type	Line
Support overhang angle	45°

4 Conclusions

In this paper, a novel strategy for multi-part AM production is proposed to save total fabrication time, thus saving energy as well. The strategy considers the characteristics of the nozzle package in AM machines that all parts do not need to be printed by keeping the same height of printed layers in each part. The nozzle package structure allows several layers in one part can be printed first, then moving to another part. The strategy includes eight steps to optimize the positions of multiple parts, using the total travel length between parts as the

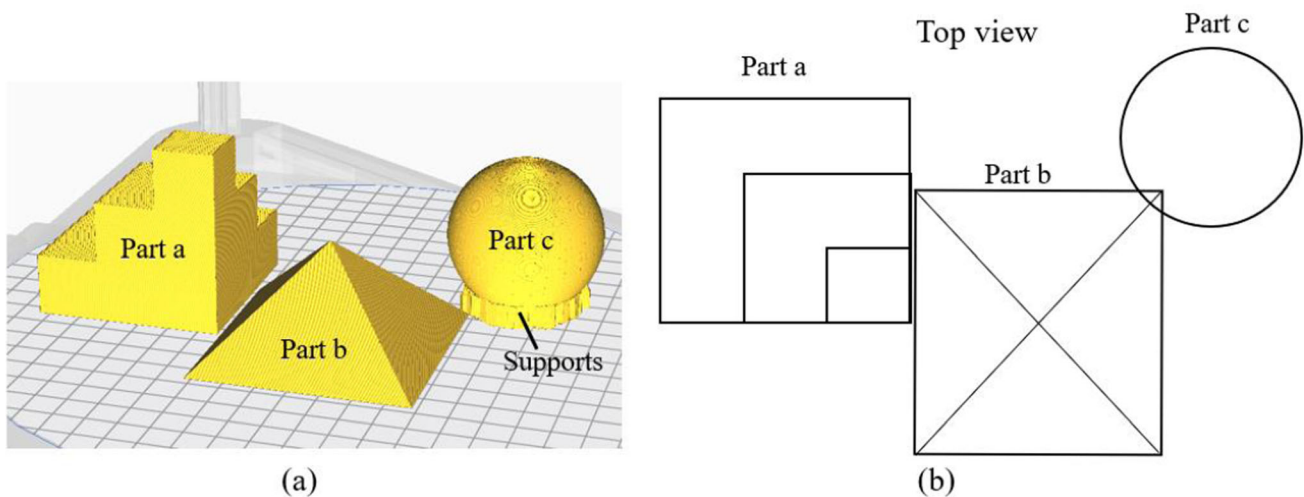
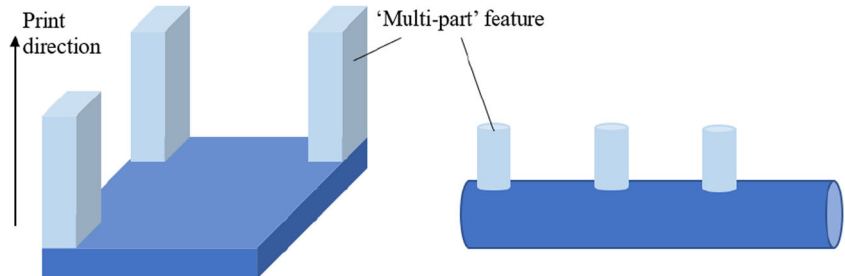


Fig. 15 Best positions of the three parts in the traditional method (a and b)

Table 2 Fabrication time estimated by using the traditional method and our strategy

Strategy	Fabrication time (s)
Traditional method in Cura 4.1.0	86400
Our strategy	86251

Fig. 16 Examples of a single part that has “multi-part” features



objective. A case study with three parts was carried out. The results show that our proposed strategy can save 149 s in terms of total fabrication time, compared with the traditional multi-part production method in Cura 4.1.0. In the future, the proposed strategy can be used for multi-part production in extrusion-based AM, with less time consumed for fabrication. Additionally, this strategy can also be used for single part fabrication if that part has “multi-part” features as shown in Fig. 16.

References

1. Fu Y-F, Rolfe B, Chiu LNS, Wang Y, Huang X, Ghabraie K (2020) Parametric studies and manufacturability experiments on smooth

- self-supporting topologies. *Virtual Phys Prototyp* 15:22–34. <https://doi.org/10.1080/17452759.2019.1644185>
2. ISO (2015) Additive manufacturing — General principles — Terminology. Iso/Astm 52900:1–26. <https://doi.org/10.1520/F2792-12A.2>
 3. Rane K, Strano M (2019) A comprehensive review of extrusion-based additive manufacturing processes for rapid production of metallic and ceramic parts. *Adv Manuf* 155–173 <https://doi.org/10.1007/s40436-019-00253-6>
 4. Bourell D, Kruth JP, Leu M, Levy G, Rosen D, Beese AM, Clare A (2017) Materials for additive manufacturing. *CIRP Ann - Manuf Technol* 66:659–681. <https://doi.org/10.1016/j.cirp.2017.05.009>
 5. Yu C, Jiang J (2020) A perspective on using machine learning in 3D bioprinting. *Int J Bioprinting* 6:4–11. <https://doi.org/10.18063/ijb.v6i1.253>
 6. Jiang J, Xu X, Stringer J (2018) A new support strategy for reducing waste in additive manufacturing. In: The 48th International Conference on Computers and Industrial Engineering (CIE 48). Auckland, pp 1–7

7. Hao L, Mellor S, Seaman O, Henderson J, Sewell N, Sloan M (2010) Material characterisation and process development for chocolate additive layer manufacturing. *Virtual Phys Prototyp* 5:57–64. <https://doi.org/10.1080/17452751003753212>
8. Bos F, Wolfs R, Ahmed Z, Salet T (2016) Additive manufacturing of concrete in construction: potentials and challenges of 3D concrete printing. *Virtual Phys Prototyp* 11:209–225. <https://doi.org/10.1080/17452759.2016.1209867>
9. Zocca A, Colombo P, Gomes CM, Günster J (2015) Additive manufacturing of ceramics: issues, potentialities, and opportunities. *J Am Ceram Soc* 98:1983–2001. <https://doi.org/10.1111/jace.13700>
10. Jiang J, Hu G, Li X, Xu X, Zheng P, Stringer J (2019) Analysis and prediction of printable bridge length in fused deposition modelling based on back propagation neural network. *Virtual Phys Prototyp* 14:253–266. <https://doi.org/10.1080/17452759.2019.1576010>
11. Jiang J, Lou J, Hu G (2019) Effect of support on printed properties in fused deposition modelling processes. *Virtual Phys Prototyp* 14: 308–315. <https://doi.org/10.1080/17452759.2019.1568835>
12. Ding D, Pan Z, Cuiuri D, Li H (2015) A practical path planning methodology for wire and arc additive manufacturing of thin-walled structures. *Robot Comput Integr Manuf* 34:8–19. <https://doi.org/10.1016/j.rcim.2015.01.003>
13. An JY, He Y, Zhong FJ et al (2014) Optimization of tool-path generation for material extrusion-based additive manufacturing technology. *Addit Manuf* 1:32–47. <https://doi.org/10.1016/j.addma.2014.08.004>
14. Jin Y, He Y, Fu G, Zhang A, du J (2017) A non-retraction path planning approach for extrusion-based additive manufacturing. *Robot Comput Integr Manuf* 48:132–144. <https://doi.org/10.1016/j.rcim.2017.03.008>
15. Muller P, Hascoet JY, Mognol P (2014) Toolpaths for additive manufacturing of functionally graded materials (FGM) parts. *Rapid Prototyp J* 20:511–522. <https://doi.org/10.1108/RPJ-01-2013-0011>
16. Ozbolat IT, Khoda AKMB (2014) Design of a new parametric path plan for additive manufacturing of hollow porous structures with functionally graded materials. *J Comput Inf Sci Eng* 14:14. <https://doi.org/10.1115/1.4028418>
17. Liu J, Ma Y, Qureshi AJ, Ahmad R (2018) Light-weight shape and topology optimization with hybrid deposition path planning for FDM parts. *Int J Adv Manuf Technol* 97:1123–1135. <https://doi.org/10.1007/s00170-018-1955-4>
18. Coupek D, Friedrich J, Battan D, Riedel O (2018) Reduction of support structures and building time by optimized path planning algorithms in multi-axis additive manufacturing. *Procedia CIRP* 67:221–226. <https://doi.org/10.1016/j.procir.2017.12.203>
19. Jiang J, Stringer J, Xu X (2019) Support optimization for flat features via path planning in additive manufacturing. *3D Print Addit Manuf* 6:171–179. <https://doi.org/10.1089/3dp.2017.0124>
20. Jiang J, Xu X, Stringer J (2019) Optimization of process planning for reducing material waste in extrusion based additive manufacturing. *Robot Comput Integr Manuf* 59:317–325. <https://doi.org/10.1016/j.rcim.2019.05.007>
21. Jiang J, Weng F, Gao S, Stringer J, Xu X, Guo P (2019) A support interface method for easy part removal in direct metal deposition. *Manuf Lett* 20:30–33. <https://doi.org/10.1016/j.mfglet.2019.04.002>
22. Zhang Y, Bernard A, Harik R, Karunakaran KP (2017) Build orientation optimization for multi-part production in additive manufacturing. *J Intell Manuf* 28:1393–1407. <https://doi.org/10.1007/s10845-015-1057-1>
23. Jiang J, Xu X, Stringer J (2019) Optimisation of multi-part production in additive manufacturing for reducing support waste. *Virtual Phys Prototyp* 14:219–228. <https://doi.org/10.1080/17452759.2019.1585555>
24. Yang Y, Fuh JYH, Loh HT, Wong YS (2003) Multi-orientational deposition to minimize support in the layered manufacturing process. *J Manuf Syst* 22:116–129
25. Thrimurthulu K, Pandey PM, Reddy NV, Venkata Reddy N (2004) Optimum part deposition orientation in fused deposition modeling. *Int J Mach Tools Manuf* 44:585–594
26. Zhao J (2005) Determination of optimal build orientation based on satisfactory degree theory for RPT. In: Proceedings - Ninth International Conference on Computer Aided Design and Computer Graphics, CAD/CG 2005. pp 225–230
27. Das P, Chandran R, Samant R, Anand S (2015) Optimum part build orientation in additive manufacturing for minimizing part errors and support structures. *Procedia Manuf* 1:343–354. <https://doi.org/10.1016/j.promfg.2015.09.041>
28. Luo Z, Yang F, Dong G et al (2016) Orientation optimization in layer-based additive manufacturing process. *Proc ASME Des Eng Tech Conf 1A–2016:1–10.* <https://doi.org/10.1115/DETC2016-59969>
29. Jiang J, Stringer J, Xu X, Zhong RY (2018) Investigation of printable threshold overhang angle in extrusion-based additive manufacturing for reducing support waste. *Int J Comput Integr Manuf* 31:961–969. <https://doi.org/10.1080/0951192X.2018.1466398>

Publisher's note Springer Nature remains neutral with regard to jurisdictional claims in published maps and institutional affiliations.